Phase Transformation of Materials

Nong-Moon Hwang

Dec. 4, 2008

Precipitate Growth

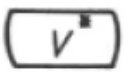

If the nucleus consists of semi-coherent and incoherent interfaces, what would be the growth shape?

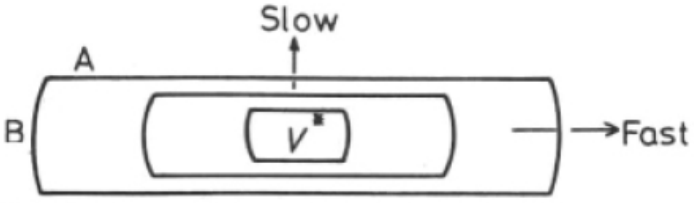

Fig. 5.13 The effect of interface type on the morphology of a growing precipitate. (A) Low-mobility semicoherent interfaces. (B) High-mobility incoherent interfaces.

→ Origin of the Widmanstätten morphology

Overall Transformation Kinetics – TTT Diagram

Transformation as a function of Time and Temperature

→ f (t,T)

Plot f vs log t.

Plot the fraction of transformation (1%, 99%) in T-log t coordinate.

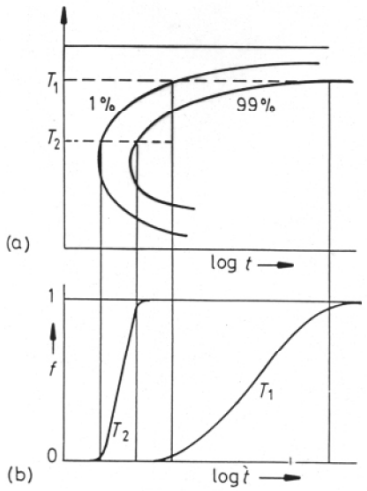

Fig. 5.23 The percentage transformation versus time for different transformation temperatures.

Overall Transformation Kinetics – TTT Diagram

Three Transformation Types

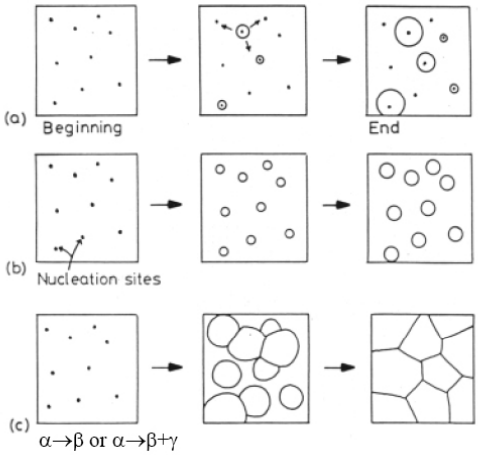

(a) continuous nucleation → f depends on the nucleation rate and the growth rate.

(b) all nuclei present at t = 0 → f depends on the number of nucleation sites and the growth rate.

(c) All of the parent phase is consumed by the transformation product. → pearlite, cellular ppt, massive transformation, recrystallization

Fig. 5.24 (a) Nucleation at a constant rate during the whole transformation. (b) Site saturation – all nucleation occurs at the beginning of transformation. (c) A cellular transformation.

Overall Transformation Kinetics – TTT Diagram

Let's derive f(t, T) in the case of a cellular transformation.

If the cells grow as spheres at a constant rate v, V of a cell nucleated at time zero is given by $V = \frac{4}{3}\pi r^3 = \frac{4}{3}\pi(vt)^3$

A cell which does not nucleate until time τ will have a volume $V' = \frac{4}{3}\pi v^3 (t-\tau)^3$

The number of nuclei that formed in dτ will be Ndτ per unit volume of untransformed α,

$$f = \sum V' = \frac{4}{3}\pi N v^3 \int_0^t (t-\tau)^3 d\tau$$

$$f_{ext} = \frac{\pi}{3} N v^3 t^4 \qquad for\ f << 1$$

valid before impingement

Overall Transformation Kinetics – TTT Diagram

Johnson-Mehl-Avrami Equation

$f_{ext} = \frac{\pi}{3} N v^3 t^4$ *for* $f << 1$ valid before impingement

How can we handle impingement?
This is a good problem of mathematics.

Hint) f : real fraction, f_{ext} : fraction without considering impingement
Find a relation between df and df_{ext}.

$df = df_{ext}(1-f)$ $\quad f = 1 - \exp\left(-\frac{\pi}{3} N v^3 t^4\right)$ $\quad f = 1 - \exp\left(-kt^n\right)$

Explanation of Experimental Results

An alloy with the composition Al-4 wt%Cu (1.7 at %) was quenched from about 540°C rapidly into water and then aged below about 180°C, the stable $CuAl_2$ did not form but the other precipitate is formed from a fcc α matrix.

Explain why and how such a thing happens?

Detailed study showed that the precipitate phase changed by following sequence with ageing time .

$$\alpha_0 \rightarrow \alpha_1 + \text{GP zone} \rightarrow \alpha_2 + \theta'' \rightarrow \alpha_3 + \theta' \rightarrow \alpha_4 + \theta\ (\mathbf{CuAl_2})$$

Note that GP zone, θ'', θ' and θ are different phases.

Guess the related thermodynamics and kinetics as much as you can.

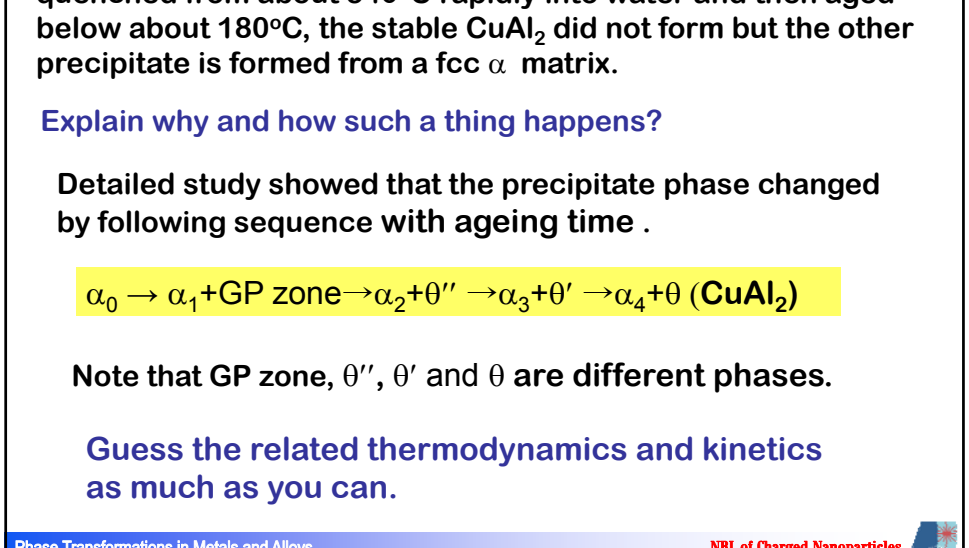

GP Zones

The zones minimize their strain energy by choosing a disc-shape perpendicular to the elastically soft <100> directions in the fcc matrix

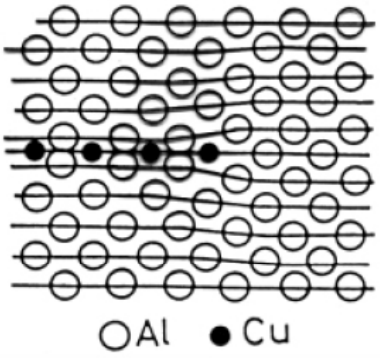

Fig. 5.26 Section through a GP zone parallel to the (200) plane. (Based on the work of V. Gerold: *Zeitschrift für Metallkunde* **45** (1954) 599.)

Precipitation in Age-Hardening Alloys

Precipitation in Aluminum-Copper Alloys

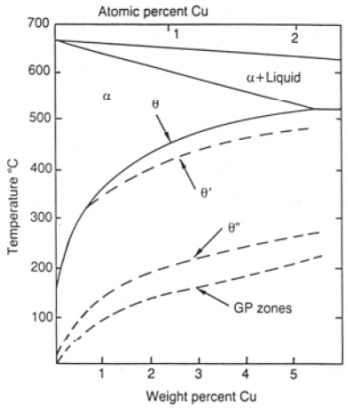

Fig. 5.25 Al-Cu phase diagram showing the metastable GP zone, Θ″ and Θ′ solvuses. (Reproduced from G. Lorimer, *Precipitation Processes in Solids*, K.C. Russell and H.I. Aaronson (Eds.), The Metallurgical Society of AMIE, 1978, p. 87.)

$\alpha_0 \rightarrow \alpha_1$+GP zones$\rightarrow\alpha_2+\theta''$
$\rightarrow\alpha_3+\theta' \rightarrow\alpha_4+\theta$ (**$CuAl_2$**)

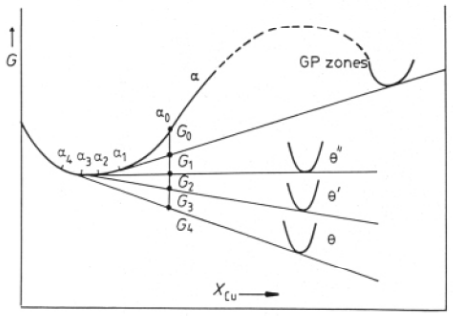

Fig. 5.27 A schematic molar free energy diagram for the Al-Cu system.

Low Activation Energy of Transition Phases

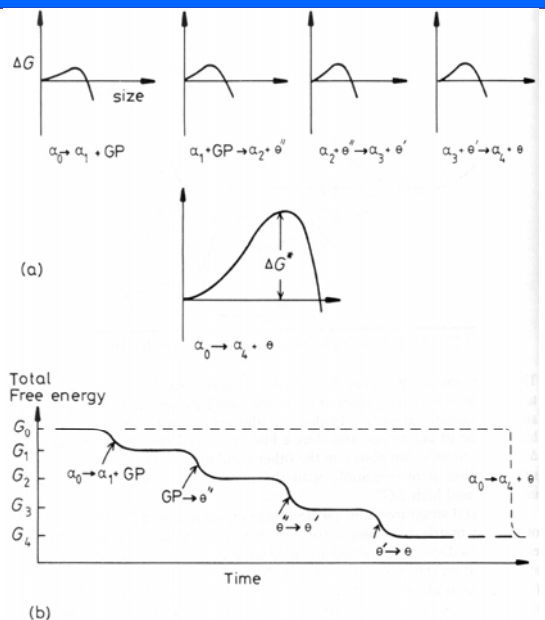

GP Zones

The Crystal Structures of θ″, θ′ and θ

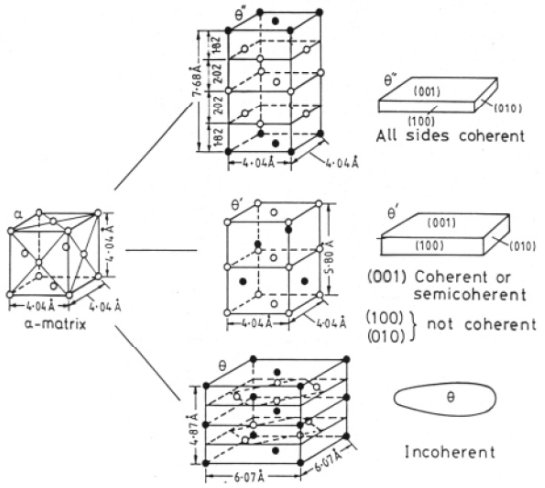

Fig. 5.29 Structure and morphology of Θ″, Θ′ and Θ in Al-Cu (○ Al, ● Cu).

GP Zones

GP zones of Al-Cu alloys x 720,000

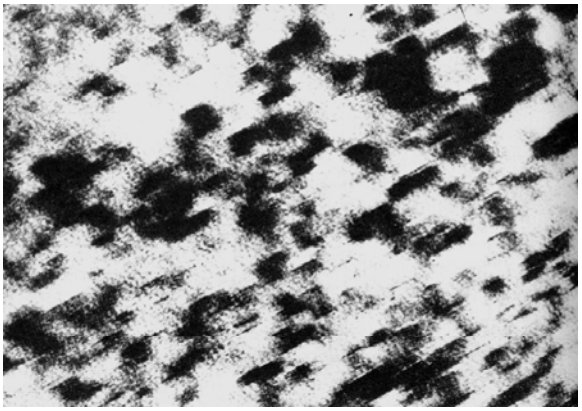

Fully coherent, about 2 atomic layers thick and 10 nm in diameter with a spacing of ~ 10 nm

GP Zones

θ″ of Al-Cu alloys x 63,000

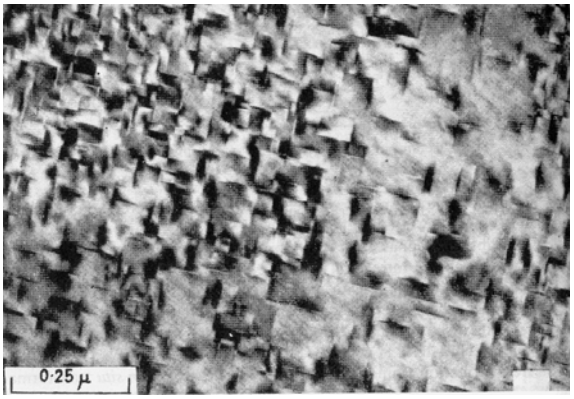

Tetragonal unit cell, essentially a distorted fcc in which Cu and Al atoms are ordered on (001) planes, fully-coherent plate-like ppt with $\{001\}_\alpha$ habit plane. ~ 10 nm thick and 100 nm in diameter.

GP Zones

θ′ of Al-Cu alloys x 18,000

θ′ has (001) planes that are identical with **$\{001\}_\alpha$ and forms as plates on $\{001\}_\alpha$ with the same orientation relationship as θ″. (100), (010) → incoherent , ~ 1 μm in diameter.**

GP Zones

θ of Al-Cu alloys x 8,000

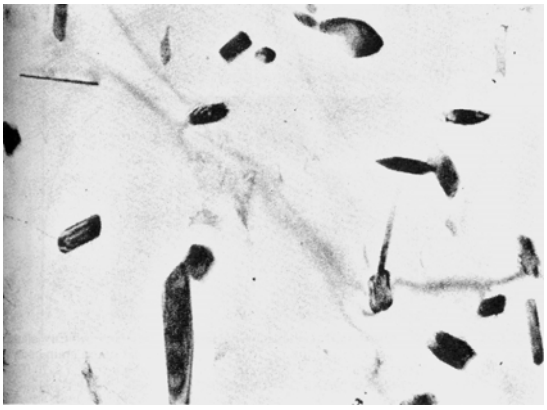

$CuAl_2$: complex body centered tetragonal, incoherent or complex semicoherent

GP Zones

Nucleation sites in Al-Cu alloys

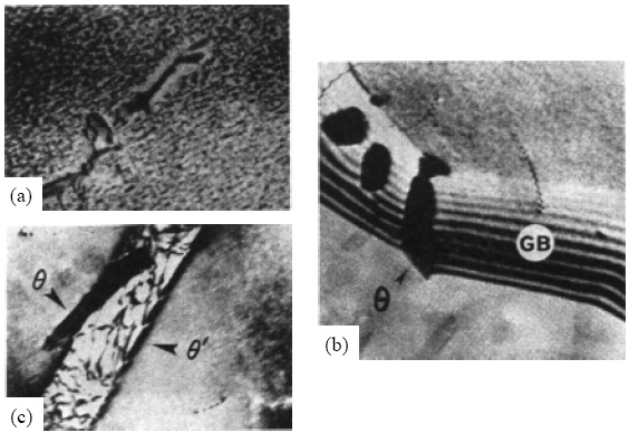

Fig. 5.31 Electron micrographs showing nucleation sites in Al-Cu alloys. (a) Θ″ → Θ′. Θ′ nucleates at dislocation (x 70,000). (b) Θ nucleation on grain boundary (GB) (x 56,000). (c) Θ′ → Θ. Θ nucleates at Θ′/matrix interface (x 70,000). (After P. Haasen, *Physical Metallurgy*, Cambridge University Press, Cambridge, 1978.)

GP Zones

The Effect of Ageing Temperature on the Sequence of Precipitates

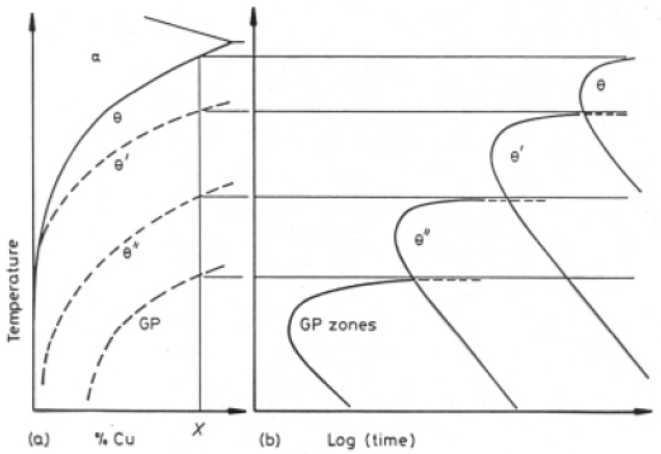

Fig. 5.32 (a) Metastable solvus lines in Al-Cu (schematic). (b) Time for start of precipitation at different temperatures for alloy X in (a).

GP Zones

The mechanism whereby a more stable precipitate grows at the expense of a less stable precipitate?

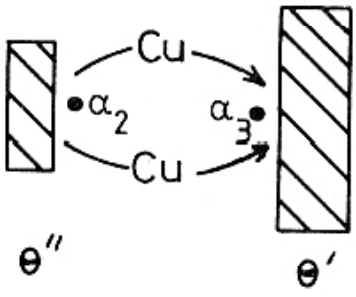

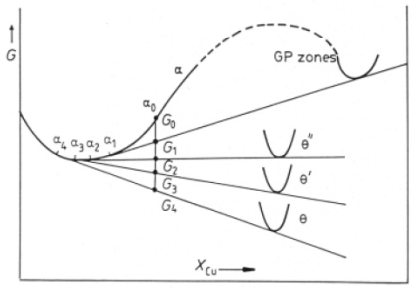

Fig. 5.27 A schematic molar free energy diagram for the Al-Cu system.

Fig. 5.33 Matrix in equilibrium with Θ″ (α_2) contains more Cu than matrix in equilibrium with Θ′ (α_3). Cu diffuses as shown causing Θ″ to shrink and Θ′ to grow.

Explanation of Experimental Results

The two microstructures show that precipitates are free near the grain boundary after being quenched and annealed.
Explain why.

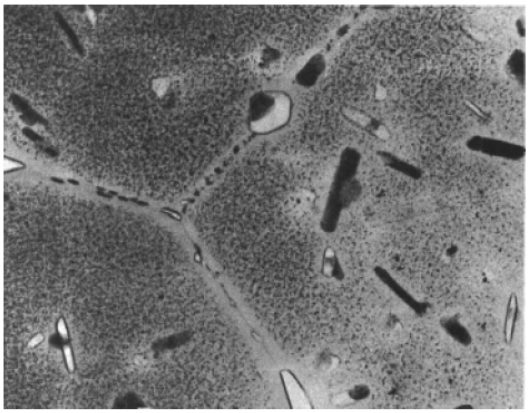

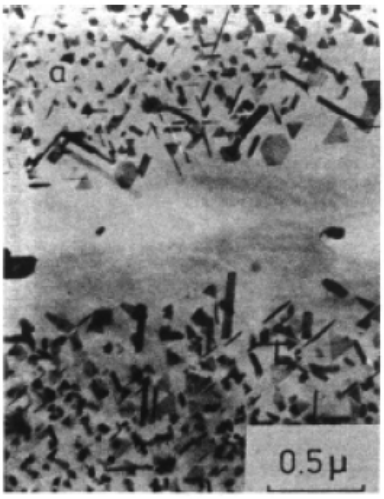

(a) Al-Zn-Mg-Cu alloy (b) Al-Ge alloy

Explanation of Experimental Results

The growth rate of GP zones is orders of magnitude higher than that predicted from the data extrapolated from the high-temperature diffusion data down to the ageing temperature.

What would be the possible reason?

Hint 1: This happens during ageing after quenching and does not happen if slowly cooled.

Hint 2: The reason for this is also related to the formation of the precipitate-free zone in Al-Ge alloy in the previous page.

If you concluded that such a high growth rate during ageing after quenching is due to the high vacancy concentration from quenched-in vacancies, how can you design an experiment to support your conclusion?

Quenched-in Vacancies

Precipitate-Free Zone(PFZ) due to Vacancy Diffusion

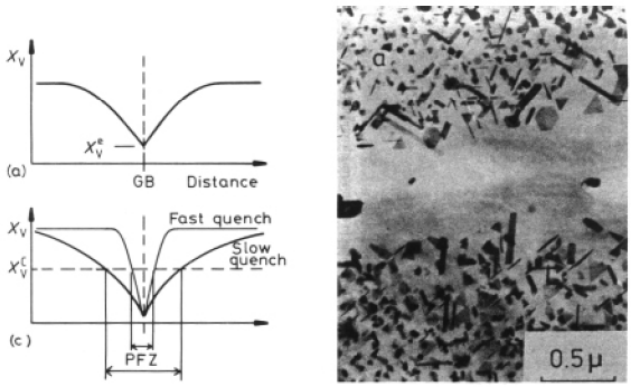

Fig. 5.35 A PFZ due to vacancy diffusion to a grain boundary during quenching. (a) Vacancy concentration profile. (b) A PFZ in an Al-Ge alloy (x 20,000). (c) Dependence of PFZ width on critical vacancy concentration X_v^c and rate of quenching. [(b) After G. Lorimer in *Precipitation in Solids*, K.C. Russell and H.I. Aaronson (Eds.), The Metallurgical Society of AIME, 1978.]

Quenched in Vacancies

PFZs can also be induced by the nucleation and growth of grain boundary precipitates during cooling from the solution treatment temperature

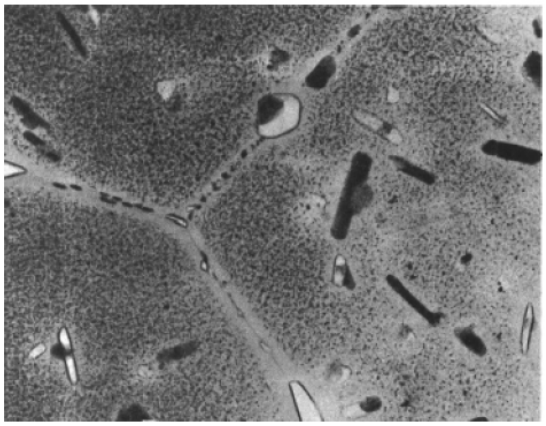

Fig. 5.36 PFZs around grain boundaries in a high-strength commercial Al-Zn-Mg-Cu alloy. Precipitates on grain boundaries have extracted solute from surrounding matrix. (x 59,200)

Age Hardening

Hardness vs. Time by Ageing

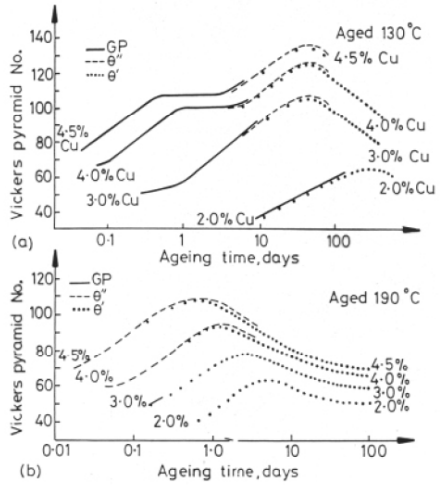

Fig. 5.37 Hardness vs. time for various Al-Cu alloys at (a) 130°C (b) 190°C. (After J.M. Silcock. T.J. Heal and H.K. Hardy, *Journal of the Institute of Metals* **82** (1953-1954) 239.

Why maximum?

Ageing at 130°C produces higher maximum hardness than ageing at 190°C.

At 130°C, however, it takes too a long time.

How can you get the high hardness for the relatively short ageing time?

Double ageing treatment first below the GP zone solvus → fine dispersion of GP zones **then ageing at higher T**

Spinodal Decomposition

Spinodal mode of transformation has no barrier to nucleation

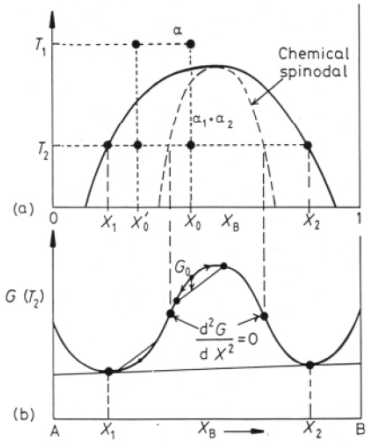

Fig. 5.38 Alloys between the spinodal points are unstable and can decompose into two coherent phases α_1 and α_2 without overcoming an activation energy barrier. Alloys between the coherent miscibility gaps and the spinodal are metastable and can decompose only after nucleation of the other phase.

How does it differ between inside and outside the inflection point of Gibbs free energy curve?

$$\frac{d^2G}{dX^2} < 0$$

If the alloy lies outside the spinodal, small variation in composition leads to an increase in free energy and the alloy is therefore metastable.

The free energy can only be decreased if nuclei are formed with a composition very different from the matrix. → nucleation and growth

Spinodal Decomposition

Composition fluctuations within the spinodal

Normal down-hill diffusion

up-hill diffusion

interdiffusion coefficient D<0

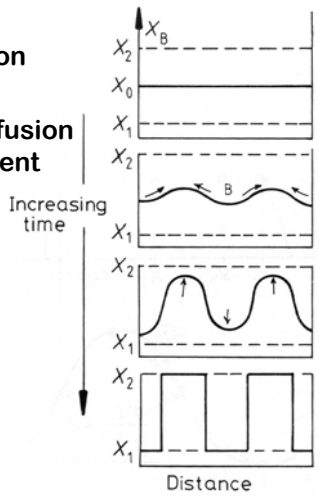

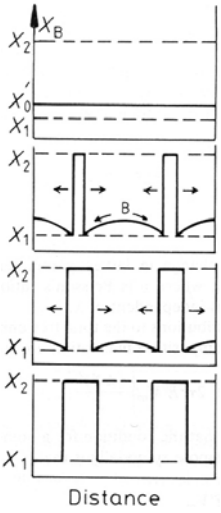

Spinodal Decomposition

Coherent Miscibility Gap

This is the line defining the equilibrium compositions of the coherent phases that result from spinodal decomposition

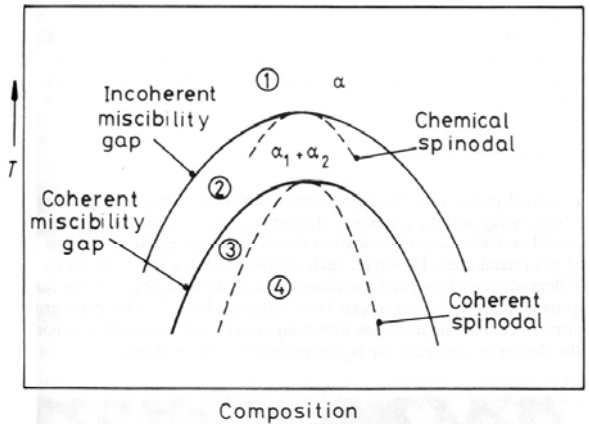

The Precipitation of Ferrite from Austenite

The Iron-Carbon Phase Diagram

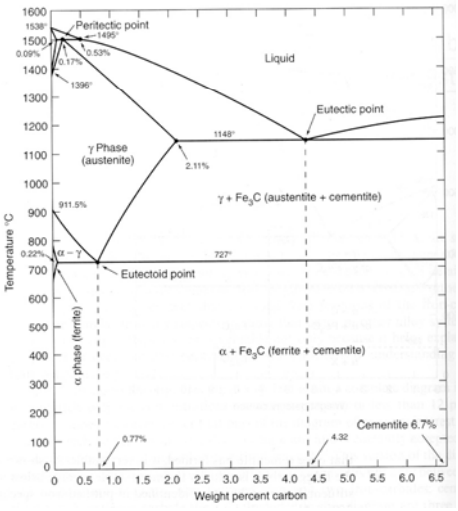

Microstructure(0.4%C) evolved by slow cooling (air, furnace) ?

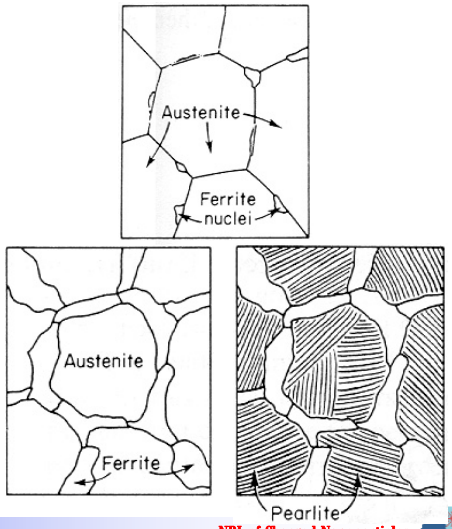

The Precipitation of Ferrite from Austenite

Diffusional Transformation of Austenite into Ferrite

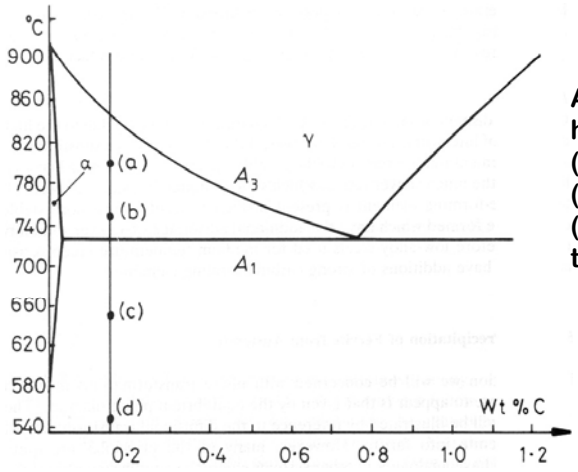

Fe-0.15%C

After being austenitized,
held at (a) 800°C for 150 s
(b) 750°C for 40 s
(c) 650°C for 9 s
(d) 550°C for 2 s and
then quenched to room T.

What would be the microstructures?

The Precipitation of Ferrite from Austenite

Microstructures of an Fe-0.15%C alloy austenitized

(c) 650°C for 9 s

(a) 800°C for 150 s

GB allotrio-morphs

(d) 550°C for 2 s

(b) 750°C for 40 s

Widmanstätten side plates (b), (c), (d)

The Precipitation of Ferrite from Austenite

Relative Velocity of Incoherent & Semicoherent Interfaces

At small undercoolings it is proposed that both semicoherent and incoherent interfaces can migrate at similar rates, while at large undercoolings only incoherent interfaces can make full use of the increased driving force.

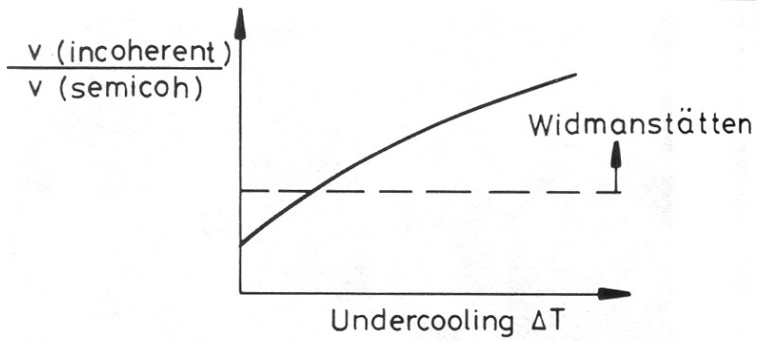

The reason for the transition from grain boundary allotriomorphs to Widmanstätten side-plates with increasing undercooling is not fully understood.

The Precipitation of Ferrite from Austenite

Typical TTT curve for γ -> α transformation

A TTT diagram for the precipitation of ferrite
in a hypoeutectoid steel will have a typical C shape.

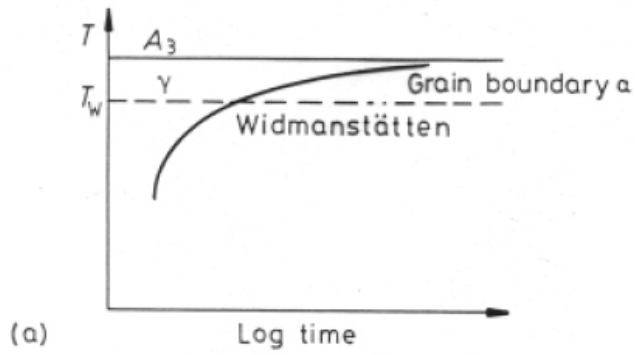

Eutectoid Transformation

Pearlite Reaction in Fe-C Alloys

$$\gamma \rightarrow \alpha + Fe_3C$$

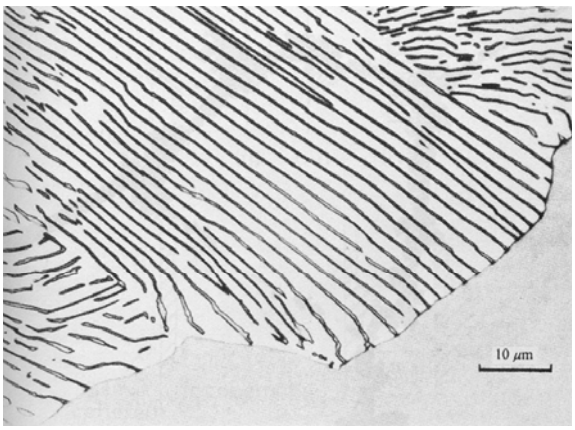

Pearlite grows into the austenite grain with which it does not have an orientation relationship.

Growth of Pearlite

Relative Positions of the Transformation curves
for Pearlite and Bainite in Plain Carbon Eutectoid Steels.

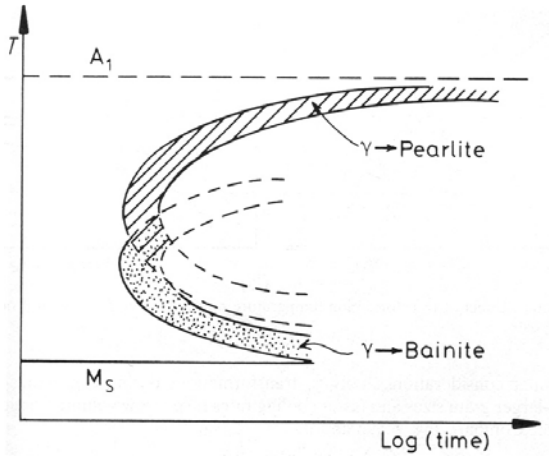

Bainite Transformation

Upper Banite in medium-carbon steel
350 ~ 550°C, laths, K-S relationship, similar to Widmanstäten plates

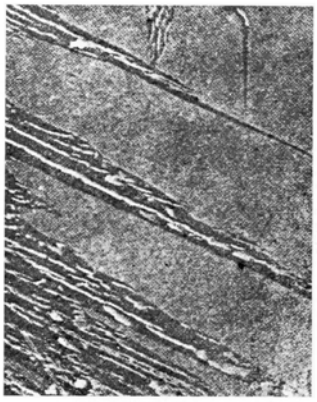

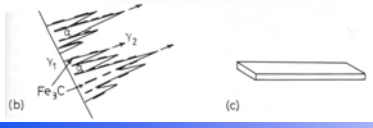

Lower Bainite
in 0.69wt% C low-alloy steel

plates with the same habit plane as that of martensite

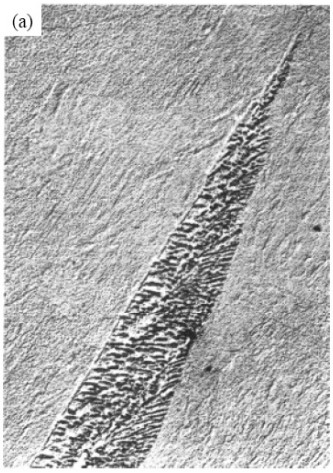

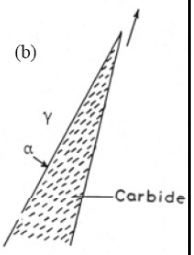

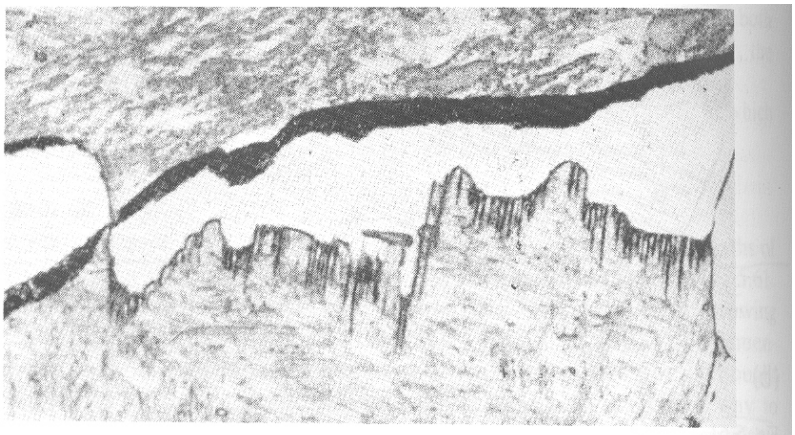

Fig. 5.62 Hypoeutectoid steel (0.6% C) partially transformed for 30 min at 710 °C, inefficiently quenched. Bainitic growth into lower grain of austenite and pearlitic growth into upper grain during quench (× 1800). (After M. Hillert in *Decomposition of Austenite by Diffusional Processes*, V.F. Zackay and H.I. Aaronson (Eds.), 1962, by permission of the Metallurgical Society of AIME.)

Pearlite : no specific orientation relationship
Bainite : orientation relationship